

## Accounts

# Magnetic Field Effects and Spin Dynamics of Radical Reactions in Solution

Hisaharu Hayashi,\* Yoshio Sakaguchi, and Masanobu Wakasa

Molecular Photochemistry Laboratory, RIKEN (The Institute of Physical and Chemical Research),  
Wako, Saitama 351-0198

(Received November 14, 2000)

A pulsed magnet which is useful for the research of chemical reactions has recently been constructed by our group. Here, the world record of the maximum magnetic field (30 T) has been attained in this research area. An optical detected X-band ESR apparatus has also been developed by our group. The world's best sensitivity and resolution have been realized in this apparatus. In this account, we review our recent results on new magnetic field effects and spin dynamics obtained with such novel methods as described above for radical reactions at room temperature in solution. In Section 1, typical mechanisms of MFEs on radical pairs such as the  $\Delta g$  mechanism and the relaxation mechanism are explained as the introduction of this review. In Section 2, the saturation of MFEs due to the  $\Delta g$  mechanism observed for radical pairs generated from the photoreduction of 4-methoxybenzophenone with benzenethiol in fluid solutions under ultrahigh fields are described. In Section 3, the saturation and reversion of MFEs due to the relaxation mechanism observed for radical pairs generated from the photoreduction of carbonyl and quinone compounds in micellar solutions under ultrahigh fields are reviewed. In Section 4, the first observation of MFEs on the reactions of three-spin systems generated photochemically in solution are introduced. In Section 5, we describe spin dynamics of radical pairs studied with our optically detected ESR apparatus for radical pairs generated from the photoreduction of carbonyl and quinone compounds in micellar solutions.

Before the early 1970's, many papers had reported magnetic field effects (MFEs) on chemical and biological reactions. Almost all of such reported data, however, had lacked reproducibility and theoretical interpretation. Thus, most scientists at that time believed that ordinary magnetic fields less than 2 T could not exert an appreciable influence on chemical and biological reactions. This idea seems reasonable because magnetic energies induced on chemical species are much smaller than those related to chemical reactions.<sup>1</sup> In the middle 1970's, however, chemical reactions through radical pairs in solution were found to be appreciably influenced by ordinary magnetic fields. These MFEs were explained by the fact that very small magnetic energies of radical pairs could switch their non-equilibrium spin conversion processes.<sup>1</sup> Such studies of MFEs on radical pair reactions together with those of chemically induced dynamic electron and nuclear polarizations (CIDEP and CIDNP) have brought about the advent of a new research field called "Spin Chemistry".<sup>2</sup>

The present review is focused on a few novel MFEs and related phenomena which have recently been investigated in our group for radical reactions generated photochemically in solution. In Section 1, typical mechanisms of MFEs on radical pairs are explained for the introduction of this review. In Section 2, MFEs due to the  $\Delta g$  mechanism observed under ultra-

high fields are described. In Section 3, MFEs due to the relaxation mechanism observed under ultrahigh fields are reviewed. In Section 4, MFEs on the reactions of three-spin systems are introduced. In Section 5, spin dynamics of radical pairs studied with our optically detected ESR apparatus are described.

### 1. Typical Mechanisms of MFEs

Figure 1 shows the reaction scheme of radical pairs produced from singlet and triplet precursors. From a singlet radical pair, a cage product and escape radicals are produced from cage recombination and escape from a solvent cage, respectively. From a triplet radical pair, however, escape radicals are usually produced. The above-mentioned processes are not influenced by magnetic fields, but the singlet–triplet (S–T) conversion of radical pairs has been found to be influenced by magnetic fields induced by external magnets, resonant microwave, and nuclear spins inside radical pairs as shown below. Thus, the radical pair lifetime and the yields of cage and escape products can be affected by magnetic fields.

Let us consider the mechanisms of the MFEs on the S–T conversion of radical pairs. In 1965, we found an anomalous hyperfine structure of the ESR spectrum of a radical pair of two iminoxyl radicals trapped in the x-irradiated single crystal of biacetyl dioxime and interpreted this anomaly by develop-

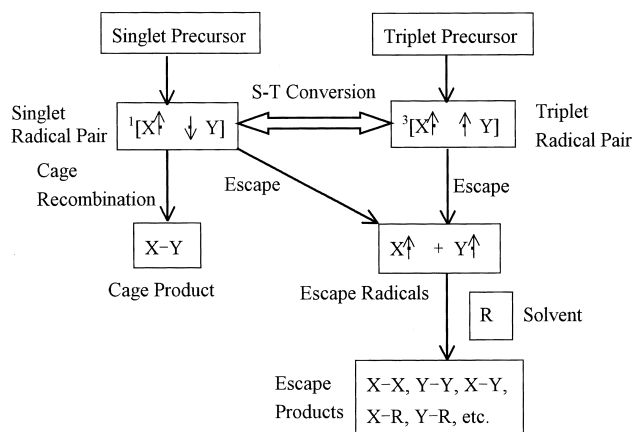


Fig. 1. Reaction scheme of radical pairs generated from singlet and triplet precursors.

ing a general theory of the spin Hamiltonian for radical pairs each of which consists of two weakly coupled radicals.<sup>3</sup> Using this general theory, we can write the spin Hamiltonian of a radical pair ( $\mathbf{H}_{\text{RP}}$ ) in solution with the exchange ( $\mathbf{H}_{\text{ex}}$ ) and isotropic magnetic ( $\mathbf{H}_{\text{mag}}$ ) terms as follows:<sup>1</sup>

$$\mathbf{H}_{\text{RP}} = \mathbf{H}_{\text{ex}} + \mathbf{H}_{\text{mag}}, \quad (1)$$

where

$$\mathbf{H}_{\text{ex}} = -J(2\mathbf{S}_1\mathbf{S}_2 + 1/2) \quad (2)$$

$$\mathbf{H}_{\text{mag}} = (g_a\mu_B S_{1z}B + \sum_i^a A_i S_{1i}I_i) + (g_b\mu_B S_{2z}B + \sum_k^b A_k S_{2k}I_k) \quad (3)$$

In Eq. 2,  $J$  is the value of the exchange integral between two electron spins ( $\mathbf{S}_1$  and  $\mathbf{S}_2$ ). In Eq. 3,  $B$  is the flux density of an external magnetic field applied along the  $z$ -axis,  $g_a$  and  $g_b$  are the isotropic  $g$ -values of two component radicals (radicals a and b) in a radical pair, respectively,  $\mu_B$  is the Bohr magneton, and  $A_i$  and  $A_k$  are the isotropic hyperfine coupling (HFC) constants with nuclear spins ( $I_i$  and  $I_k$ ) in radicals a and b, respectively.

The energies ( $E(S)$  and  $E(T_n)$ ) of the singlet and triplet radical pairs ( $|S, \chi_N\rangle$  and  $|T_n, \chi_N\rangle$ ) can be given as follows:<sup>1</sup>

$$E(S) = \langle S, \chi_N | \mathbf{H}_{\text{ex}} + \mathbf{H}_{\text{mag}} | S, \chi_N \rangle = J \quad (4)$$

$$\begin{aligned} E(T_n) &= \langle T_n, \chi_N | \mathbf{H}_{\text{ex}} + \mathbf{H}_{\text{mag}} | T_n, \chi_N \rangle \\ &= -J + ng\mu_B B + \frac{n}{2} (\sum_i^a A_i M_i + \sum_k^b A_k M_k) \end{aligned} \quad (5)$$

Here,  $\chi_N$  is the nuclear wavefunction of the radical pairs,  $n = +1, 0$ , and  $-1$ ;  $g = (g_a + g_b)/2$ . The S-T conversion between  $|S, \chi_N\rangle$  and  $|T_n, \chi_N\rangle$  occurs through the following off-diagonal matrix elements:<sup>1</sup>

$$\begin{aligned} \langle T_0, \chi_N | \mathbf{H}_{\text{ex}} + \mathbf{H}_{\text{mag}} | S, \chi_N \rangle \\ = \frac{1}{2} [\Delta g \mu_B B + (\sum_i^a A_i M_i - \sum_k^b A_k M_k)] = \hbar Q_N \end{aligned} \quad (6)$$

$$\langle T_{\pm 1}, \chi_N | \mathbf{H}_{\text{ex}} + \mathbf{H}_{\text{mag}} | S, \chi_N \rangle = \frac{\mp A_i}{2\sqrt{2}} [I_i(I_i+1) - M_i(M_i \mp 1)]^{1/2} \quad (7)$$

Here,  $\Delta g = (g_a - g_b)/2$ ,  $M_i$  (for  $|\chi_N'\rangle = |M_i', M_k'\rangle = M_i \mp 1$

(for  $|\chi_N\rangle = |M_i, M_k\rangle$ ), and  $M_k' = M_k$ .

Figure 2 shows the magnetic field dependence of the S-T conversion of a radical pair for (a) the  $\Delta g$  mechanism ( $\Delta gM$ ), (b) the hyperfine coupling mechanism (HFCM), and (c) the level-crossing mechanism (LCM), respectively. When the  $\Delta g$  value is not zero, but when the  $J$ ,  $A_i$ , and  $A_k$  values are zero, the  $\Delta gM$  is applicable. In this mechanism, the S-T<sub>0</sub> conversion rate is increased through the  $\Delta g\mu_B B$  term of Eq. 6 with increasing  $B$  as shown in Fig. 2a.<sup>1</sup> When the  $A_i$  and/or  $A_k$  values are not zero, but when the  $J$  and  $\Delta g$  values are zero, the HFCM is applicable. In this mechanism, the S-T<sub>n</sub> ( $n = +1, 0$ , and  $-1$ ) conversions are possible at zero field through the  $(\sum_i^a A_i M_i - \sum_k^b A_k M_k)$  term of Eq. 6 and the right side of Eq. 7. In the presence of a magnetic field, however, only the S-T<sub>0</sub> conversion becomes possible as shown in Fig. 2b. Thus, the S-T conversion rate is reduced by the field in the case of the HFCM.<sup>1</sup> When the  $J$  and  $A_i$  (or  $A_k$ ) values are not zero, the LCM is applicable. In this mechanism, the S-T<sub>n</sub> ( $n = 1, 0$ , and  $-1$ ) conversions are not possible at zero field, because the S and  $T_n$  states are separated by  $|2J|$  at zero field as shown in Fig. 2c. On the other hand, the S-T<sub>-1</sub> (in the case of  $J < 0$  J) or S-T<sub>+1</sub> (in the case of  $J > 0$  J) conversion becomes possible through the right side of Eq. 7 at the level-crossing field ( $B_{\text{LC}}$ ).

$$B_{\text{LC}} = |2J|/g\mu_B \quad (8)$$

At this field, the S-T<sub>-1</sub> (or S-T<sub>+1</sub>) conversion is suddenly in-

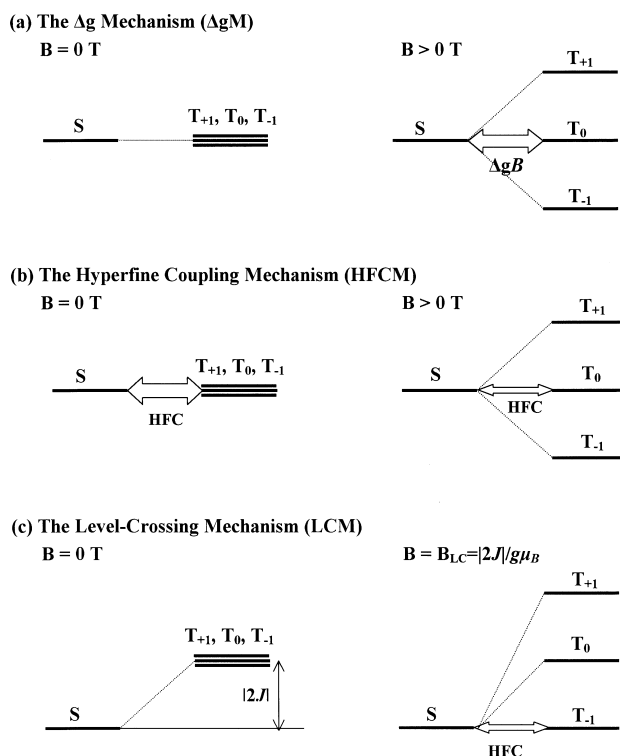


Fig. 2. Conversion between the singlet ( $S$ ) and triplet ( $T_n$ ,  $n = 1, 0, -1$ ) states of a radical pair in the absence and presence of a magnetic field: (a) The  $\Delta g$  mechanism ( $\Delta gM$ ); (b) The hyperfine coupling mechanism (HFCM); (c) The level-crossing mechanism (LCM).

creased as shown in Fig. 2c.<sup>1</sup>

It is noteworthy that the S–T<sub>0</sub> conversion rate is given by  $Q_N$  for a radical pair with  $J \sim 0$  J.<sup>1</sup> When  $J \sim 0$  J,  $\Delta g = 0.01$ ,  $B = 1$  T, and  $A_i/g\mu_B = A_k/g\mu_B = 0$  T, the rate becomes  $4.4 \times 10^8$  s<sup>-1</sup> from Eq. 6. If such S–T<sub>0</sub> conversion rate is comparable to the escape rate of two radicals from a solvent cage, appreciable MFEs can be observed. In some cases, this condition can be satisfied in homogeneous solvents. If two radicals are confined with membranes, micelles, or chemical bonds, the escape rate of the two radicals becomes much smaller than the S–T<sub>0</sub> conversion rate. In this case, the S and T<sub>0</sub> states attain equilibrium and the T<sub>±1</sub>–T<sub>0</sub> and T<sub>±1</sub>–S relaxations become important as shown in Fig. 3. In 1984, we proposed the relaxation mechanism (RM)<sup>4</sup> in order to explain MFEs and magnetic isotope effects (MIEs) on chemical reactions in confined systems. When  $k_{ST}(0 \text{ T}), k_{ST}(B) \gg k_P$  in the RM, the decay ( $RP(t)$ ) of a radical pair produced from a triplet precursor can be represented as follows:<sup>4</sup>

$$(a) B = 0 \text{ T: } RP(t) = R_0 \exp(-k_0 t) \quad (9)$$

$$(b) B > 0 \text{ T: } RP(t) = R_F \exp(-k_F t) + R_S \exp(-k_S t) \quad (10)$$

Here,

$$k_0 = k_P/4 + k_E \quad (11)$$

$$k_F = k_P/2 + k_S \quad (12)$$

$$k_S = k_R + k_R' + k_E \quad (13)$$

The rate constants in Eqs. 9–13 are represented in Fig. 3.

Because the fast component of Eq. 10 often overlaps with the decay of triplet precursors, the observed PR-lifetimes ( $\tau_{RP}$ ) usually correspond to  $1/k_0$  (at  $B = 0$  T) and  $1/k_S$  ( $B > 0$  T). In Eqs. 11–13, the  $k_P$  and  $k_E$  values should be independent of  $B$ , but the  $k_R$  and  $k_R'$  values should be dependent of  $B$  as follows:

$$k_R = \sum_i \frac{1}{\hbar^2} \langle T_{\pm 1} | \delta H_i | T_0 \rangle^2 \frac{2\tau_i}{1 + \omega_0^2 \tau_i^2} \quad (14)$$

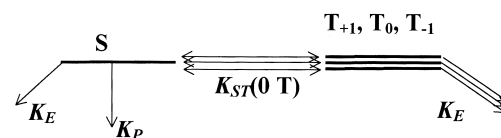
$$k_R' = \sum_i \frac{1}{\hbar^2} \langle T_{\pm 1} | \delta H_i | S \rangle^2 \frac{2\tau_i}{1 + \omega_0^2 \tau_i^2} \quad (15)$$

Here, each  $\delta H_i$  term is due to each of the dipole–dipole interaction between two components radicals, the anisotropic Zeeman terms of the two radicals, and their anisotropic HFC terms,  $\tau_i$  is each rotational correlation time, and  $\omega_0$  is given by  $g\mu_B B/\hbar$ .<sup>4</sup>

## 2. MFEs due to the $\Delta g$ Mechanism Observed under Ultra-high Fields

We have been studying MFEs and MIEs on photochemical reactions in solution since 1976. In 1976, we studied MFEs on the singlet sensitized photodecomposition of dibenzoyl peroxide at room temperature in toluene with a small superconducting magnet whose maximum field was 4.3 T.<sup>5</sup> We found that the yields of the cage and escape products were appreciably changed by the fields and that the magnetically induced changes were proportional to  $B^{1/2}$ . We interpreted such MFEs in terms of the  $\Delta g$ M. Thereafter, we started to measure dynamic

(a)  $B = 0$  T



(b)  $B > 0$  T

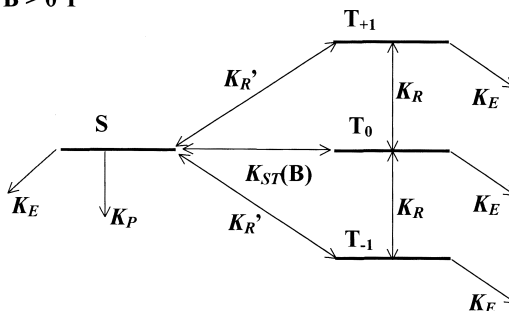


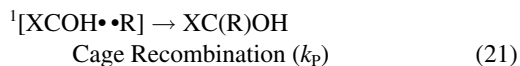
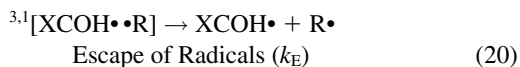
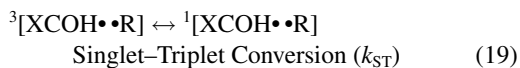
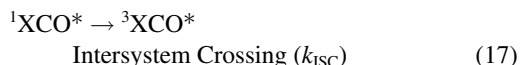
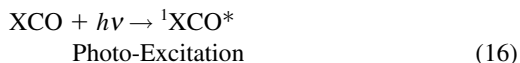
Fig. 3. Schematic diagram of the relaxation mechanism for the singlet (S) and triplet ( $T_n$ ,  $n = 1, 0, -1$ ) states of a radical pair with  $J = 0$  and rate constants ( $k_i$ ) concerning the states: (a) In the absence of a magnetic field; (b) In the presence of a magnetic field.

behavior of radical pairs, using an ns-laser photolysis apparatus and an electromagnet whose maximum field was 1.34 T. In 1993, we made an ns-laser photolysis apparatus with a double-beam probe light system, using a superconducting magnet which had the maximum field of 10 T and a room temperature bore of 50 mm.<sup>6</sup> In 1997, we also constructed a water-cooled pulsed magnet whose maximum field was 30 T.<sup>7</sup> This field was about twice as high as the previous world record (17.5 T)<sup>8</sup> which had been used for the research of MFEs on chemical reactions. Because this pulsed magnet had enough space at room temperature (a bore of 23 mm) and a fairly high repetition rate (1 shot/3 min.), we could perform precise measurements of MFEs on photochemical reactions in solution together with a double-beam probe light system and signal accumulation. Using these magnets, we have been studying the effects of ultrahigh magnetic fields on photochemical reactions in solution.

According to the  $\Delta g$ M, it has been believed that the magnetically induced changes due to the  $\Delta g$ M should be saturated at high enough fields. In almost all reactions which have hitherto been investigated for MFEs, however, good linear relationships between the magnetically induced changes due to the  $\Delta g$ M and  $B^{1/2}$  have been obtained.<sup>9</sup> In 1982, Boxcer et al. studied MFEs of photosynthetic reaction centers where radical pairs are confined to the membrane. They found with magnetic fields of up to 5 T that the MFEs were deviated from the linear relationship with  $B^{1/2}$  at 5 T.<sup>10</sup> Schulten and Edstein, however, predicted that the saturation of MFEs due to the  $\Delta g$ M should occur at extremely large fields of the order of  $10^3$  T for  $\Delta g$  values of the order of 0.01 in nonviscous solutions.<sup>11</sup> Such ultrahigh fields as  $10^3$  T can not be realized on the earth. We, therefore, have challenged their prediction and tried to find saturation behavior of the MFEs due to the  $\Delta g$ M with our apparatus. We have found that the MFEs on the escape radical yield observed with

the pulsed magnet for the photoreduction of 4-methoxybenzophenone with thiophenol (benzenethiol) in fluid solutions are saturated by the fields of  $\sim 30$  T.<sup>9</sup>

The reaction scheme of the photoreduction of a carbonyl or quinone molecule (XCO) with a hydrogen donor (RH) is represented by the following reactions:



The triplet and singlet radical pairs are represented by  ${}^3[\text{A}\cdot\cdot\text{B}]$  and  ${}^1[\text{A}\cdot\cdot\text{B}]$ , respectively, and  $k_i$  shows the respective rate constant. In this reaction, XCO and RH are 4-methoxy-benzophenone and thiophenol, respectively.

From the ns-laser photolysis measurements with the electromagnet, the superconducting magnet, or the pulsed one, we observed the time profiles ( $A(t)$ ) of the transient absorption of the ketyl radical and obtained the MFEs ( $R(B) = Y_{\text{E}}(B)/Y_{\text{E}}(0 \text{ T})$ ) on the yield of the escape radical ( $Y_{\text{E}}$ ).<sup>9</sup> The  $R(B)$  values obtained at room temperature in 2-methyl-1-propanol are plotted against  $B^{1/2}$  in Fig. 4a. As is clear from this  $R(B)$ – $B^{1/2}$  relationship, we can see that the magnetically induced change ( $1 - R(B)$ ) starts to deviate from the linear relationship between  $1 - R(B)$  and  $B^{1/2}$  above 4 T and that the change attains a saturated value above 20 T. To the best of our knowledge, this is the first observation of the saturation of the MFEs due to the  $\Delta g\text{M}$ .

We tried quantitative analysis of our results with the diffusion model presented by Freed and Pedersen as follows:<sup>12</sup>

$$R(B) = 1 - pF^* \quad (22)$$

Here,  $p$  is the initial population of the  $T_0$  level and  $F^*$  is the probability of forming the geminate product from a triplet precursor. They gave the following equation for  $F^*$ :

$$F^* = \frac{\frac{\sqrt{qB}}{2} \left[ 1 + \frac{1}{2} \ln(1 + \sqrt{qB}) \right]}{1 + \frac{\sqrt{qB}}{2} [1 + \sqrt{qB}]} \quad (23)$$

In the above equation,  $q$  is given as follows:

$$q = \Delta g \mu_B d^2 / 2\hbar D \quad (24)$$

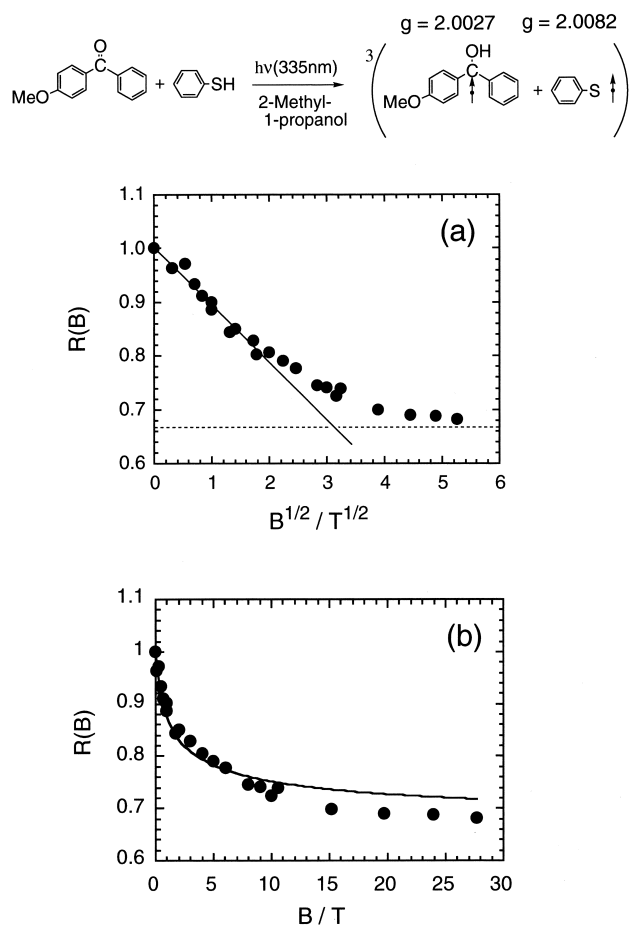


Fig. 4. (a)  $R(B)$  ( $= Y_{\text{B}}(B)/Y_{\text{E}}(0 \text{ T})$ ) values (●) obtained with our electromagnet, our superconducting magnet, and our pulsed magnet from the time profiles of the absorbance ( $A(t)$  profiles) at 550 nm for the photoreduction of 4-methoxybenzophenone with thiophenol at room temperature in 2-methyl-1-propanol. Here,  $R(B)$  values are plotted against  $B^{1/2}$ . (b)  $R(B)$  values (●) observed for the photoreduction of 4-methoxybenzophenone with thiophenol at room temperature in 2-methyl-1-propanol and their simulation (—) with Eqs. 22–25.

Here,  $d$  is the distance of closest approach of two radicals and  $D$  is the sum of the diffusion coefficients for the two radicals.

We noticed a problem in Eq. 22 because the  $p$  value should depend on  $B$  from 0 to 30 T. Thus, we assumed the following  $B$ -dependence of  $p(B)$  from the triplet mechanism presented by Atkins:<sup>13</sup>

$$R(B) = 1 - p(B)F^* = 1 - \left( \frac{1}{3} - \kappa \frac{D_{\text{ZFS}}}{B} \right) F^* \quad (25)$$

Here,  $\kappa$  is the relative anisotropy of the intersystem crossing rate and  $D_{\text{ZFS}}$  ( $= 3Z/2$ ) is the zero-field splitting of  ${}^3\text{XCO}^*$ . Because the  $D_{\text{ZFS}}$  value had not yet been obtained for 4-methoxybenzophenone, we measured the ESR spectrum of its triplet state at 77 K. From this measurement, we obtained its  $D_{\text{ZFS}}$  value as 2.7 GHz.<sup>9</sup>

By the least-squares method with Eq. 25, we analyzed our experimental data on the  $R(B)$  values in various nonviscous solutions.<sup>9</sup> Here, the  $\kappa$  value was obtained to be 0.38, from

which the  $p(0\text{ T})$  and  $p(30\text{ T})$  values were estimated to be 0.19 and 0.33, respectively. From this analysis, we have obtained the  $q$  value for each solution. From the Stokes–Einstein relation, the  $D$  value is represented by

$$D = D_1 + D_2 \quad (26)$$

$$D_1 \sim D_2 \sim kT/6\pi\eta R \quad (27)$$

Here,  $\eta$  is the solvent viscosity and  $R$  is the radius of the sphere. From Eqs. 24, 26, and 27, we can see that  $q$  becomes proportional to  $\eta$ .

$$q = \frac{\Delta g \mu_B d^2}{2\hbar D} = \frac{\Delta g \mu_B d^2 3\pi R}{2\hbar kT} \eta \quad (28)$$

Plotting the obtained  $q$  values against  $\eta$ , we found that  $q$  had a good linear relationship with  $\eta$ . The slope was obtained to be  $0.338 \times 10^3\text{ T}^{-1}/\text{cP}$ . Taking  $\Delta g = 0.0055$  and  $d = 6 \times 10^{-10}\text{ m}$ , we obtained the  $R$  value to be  $16.7 \times 10^{-10}\text{ m}$ . With this  $R$  value and Eq. 27, the  $D_i$  ( $i = 1$  or  $2$ ) value can be estimated to be  $1.29 \times 10^{-10}\text{ m}^2\text{ s}^{-1}$  at  $\eta = 1\text{ cP}$ . This  $D_i$  value is somewhat smaller than the value ( $\sim 5 \times 10^{-10}\text{ m}^2\text{ s}^{-1}$  at  $\eta = 1\text{ cP}$ ) obtained by Terazima et al. for the benzophenone ketyl radical with the transient grating method.<sup>14</sup> Although the  $R$  value of the 4-methoxy-benzophenone ketyl radical should be a little larger than that of the benzophenone ketyl radical, this discrepancy may be due to the fact that we used several approximations for the analysis of our experimental data.

Because the lifetimes of radical pairs consisting of neutral radicals have an order of 1 ns, the MFEs on the lifetimes can not be measured by ns-lasers. Recently, we have started to measure such MFEs with a ps-laser and successfully observed the MFEs in the sub-ns region for the above-mentioned reaction.<sup>15</sup>

### 3. MFEs due to the Relaxation Mechanism Observed under Ultrahigh Fields

In 1981, we found large MFEs and MIEs on the radical pair lifetime ( $\tau_{\text{RP}}$ ) and the escape radical yield ( $Y_{\text{E}}$ ) under magnetic fields of 0–70 mT with an ns-laser photolysis at room temperature for the photoreduction reactions of benzophenone (BP), benzophenone- $d_{10}$  (BP- $d_{10}$ ), and [carbonyl- $^{13}\text{C}$ ]benzophenone (BP- $^{13}\text{C}$ ) in micellar sodium dodecyl sulfate (SDS) solutions.<sup>16</sup> Here, micellar molecules act as hydrogen donors (RH). The scheme of such photoreduction reactions of the benzophenone isotopes (XCO) can also be represented by reactions 16–21. It is noteworthy that the MFEs and MIEs on  $\tau_{\text{RP}}$  can be measured with ns-lasers for the reactions in such confined systems as radical pairs in micelles and biradicals in nonviscous solvents.

From the  $A(t)$  profiles observed with an ns-laser photolysis for the generated ketyl radicals (XCOH•), we obtained remarkable MFEs and MIEs on the  $\tau_{\text{RP}}$  and  $Y_{\text{E}}$  values.<sup>16</sup> Because their MFEs and MIEs were not saturated at 70 mT, we extended the maximum field to 1.34 T with an electromagnet and obtained their MFEs and MIEs as shown in Fig. 5.<sup>4,17</sup> From Fig. 5, we can see the following new MFEs and MIEs under high fields of up to 1.34 T: (1) For the reactions of the BP isotopes in the SDS micellar solution, the  $\tau_{\text{RP}}$  and  $Y_{\text{E}}$  values increase with increasing  $B$  from 0 T to 1.34 T. These MFEs can not be

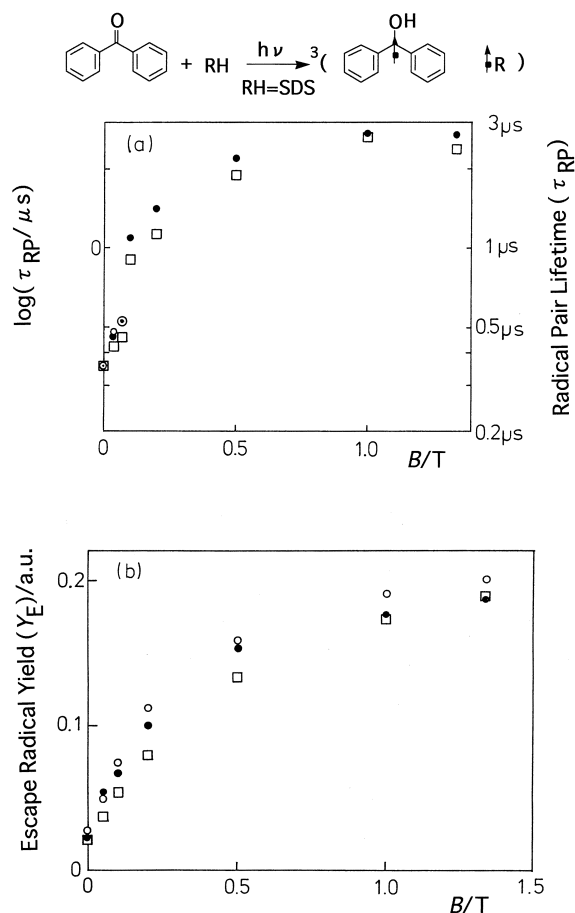


Fig. 5. MFEs and MIEs on the radical pair lifetime ( $\tau_{\text{RP}}$ ) and the escape radical yield ( $Y_{\text{E}}$ ) observed under magnetic fields of 0–1.34 T with an ns-laser photolysis at room temperature for the photoreduction reactions of (●) BP, (○) BP- $d_{10}$ , and (□) BP- $^{13}\text{C}$  in micellar sodium dodecyl sulphate (SDS) solutions.

explained by the  $\Delta g\text{M}$ , because the MFEs due to the  $\Delta g\text{M}$  for reactions from triplet precursors should decrease with increasing  $B$  from 0 T.<sup>1,4</sup> (2) These increases in the MFEs seem to approach their saturated values at  $B = 1.34\text{ T}$ . It is noteworthy that these increases do not show saturation at  $B \sim 0.1\text{ T}$ , where the MFEs due to the HFCM should be saturated. (3) Clear MIEs on the  $\tau_{\text{RP}}$  and  $Y_{\text{E}}$  values can be observed for present reactions. At each field, we can see the following order for the MIFs: BP- $^{13}\text{C} < \text{BP} < \text{BP-}d_{10}$ . (4) These MIEs are very small at  $B = 0\text{ T}$ , but they increase with increasing  $B$  from 0 T to 0.2 T. With increasing  $B$  from 0.2 T to 1.34 T, however, these MIEs decrease again. It is noteworthy that these MIEs can not be explained by the HFCM, because the MIEs due to the HFCM should decrease with increasing  $B$  from 0 T.<sup>1,4</sup>

Because the observed MFEs and MIEs on  $\tau_{\text{RP}}$  and  $Y_{\text{E}}$  at such high fields (0–1.34 T) could not be explained by the ordinary  $\Delta g\text{M}$  and HFCM, we proposed the RM in 1984 and succeeded in interpreting such novel MFEs and MIEs.<sup>4</sup> In 1997, however, Tanimoto et al. reported that they had found no MIE on  $\tau_{\text{RP}}$  for the same reactions of the benzophenone isotopes.<sup>18</sup> They have recently realized their mistakes and confirmed our results on the existence of the MIEs in these reactions.<sup>19</sup>

Using our superconducting and pulsed magnets, we have been studying the effects of ultrahigh magnetic fields on the  $\tau_{RP}$  and  $Y_E$  values at room temperature for the photoreduction of carbonyl and quinone compounds (XCO) in micelles. We have used benzophenone (BP), decafluorobenzophenone (DFBP), and 1,4-naphthoquinone (NQ) for carbonyl compounds. We have used sodium dodecyl sulfate (SDS) and  $\alpha$ -dodecyl- $\omega$ -hydroxypolyoxyethylene (Brij 35) for micelles. The scheme of such photoreduction reactions of XCOs can also be represented by reactions 16–21. From the  $A(t)$  profiles observed with an ns-laser photolysis for the generated ketyl or semiquinone radicals (XCOH $\cdot$ ), we have obtained the MFES on the  $\tau_{RP}$  and  $Y_E$  values as shown in Fig. 6.<sup>20</sup>

From Fig. 6, we can see the following new MFES under ultrahigh fields of up to 30 T: (1) For the reaction of BP in the SDS micellar solution, the  $\tau_{RP}$  value increases with increasing  $B$  from 0 T to 2 T and the value shows saturation with increasing  $B$  from 2 T to 29.6 T. (2) For the reaction of BP in the Brij 35 micellar solution, the  $\tau_{RP}$  value increases with increasing  $B$  from 0 T to 2 T, but the value decreases with increasing  $B$  from 2 T to 25 T. With increasing  $B$  from 25 T to 29.6 T, the value is almost saturated. (3) For the reaction of DFBP in the Brij 35 micellar solution, the  $\tau_{RP}$  value increases with increasing  $B$  from 0 T to 2 T and the value decreases with increasing  $B$  from 2 T to 24.6 T. With increasing  $B$  from 24.6 T to 28.7 T, the value is nearly saturated. (4) For each of the above-mentioned re-

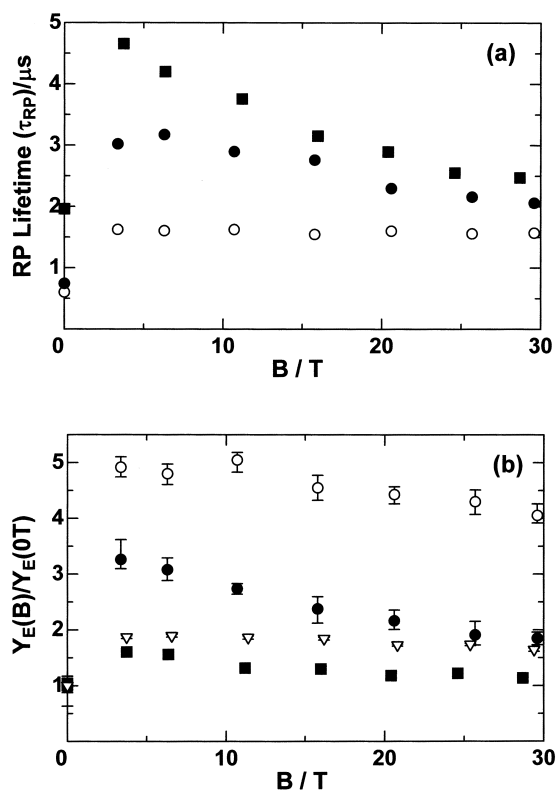


Fig. 6. The MFES on the  $\tau_{RP}$  and  $Y$  values observed for the photoreduction at room temperature: (○) of BP in an SDS micellar solution, (●) of BP in a Brij 35 micellar solution, (■) DFBP in a Brij 35 micellar solution, and (▽) of NQ in an SDS micellar solution.

actions, the  $Y_E$  value increases with increasing  $B$  from 0 T to 2 T, but the value decreases with increasing  $B$  from 2 T to about 30 T. (5) For the reaction of NQ in the SDS micellar solution, the  $Y_E$  value shows MFES similar to those observed in (4).

We could successfully reproduce the observed saturation and reversion of the  $\tau_{RP}$  values at 2 T as well as the observed saturation of the values around 30 T, using the simulation with Eqs. 9–15 of the RM. The details of the simulation will be published in the near future.<sup>21</sup> The MFES on the  $Y_E$  values could be explained by a combination of the RM and the  $\Delta gM$ . Especially, we have found that the slight decreases in  $Y$  observed with increasing  $B$  from 2 T to around 30 T are also affected by the  $\Delta gM$ .<sup>21</sup>

#### 4. MFES on the Reactions of Three-Spin Systems

Ordinary MFES on chemical reactions through radical pairs<sup>1</sup> and biradicals<sup>22</sup> are due to the spin conversion between their singlet-triplet states. Recently, we have first found large MFES with our ns-laser photolysis apparatus in several reaction systems where three odd electrons appear.<sup>23,24</sup> At first, we studied the electron transfer reaction of triplet 10-methylphenothiazine ( $^3D^*$ ) with 4-(4-cyanobenzoyloxy)TEMPO ( $^2A-R_1\cdot$ )

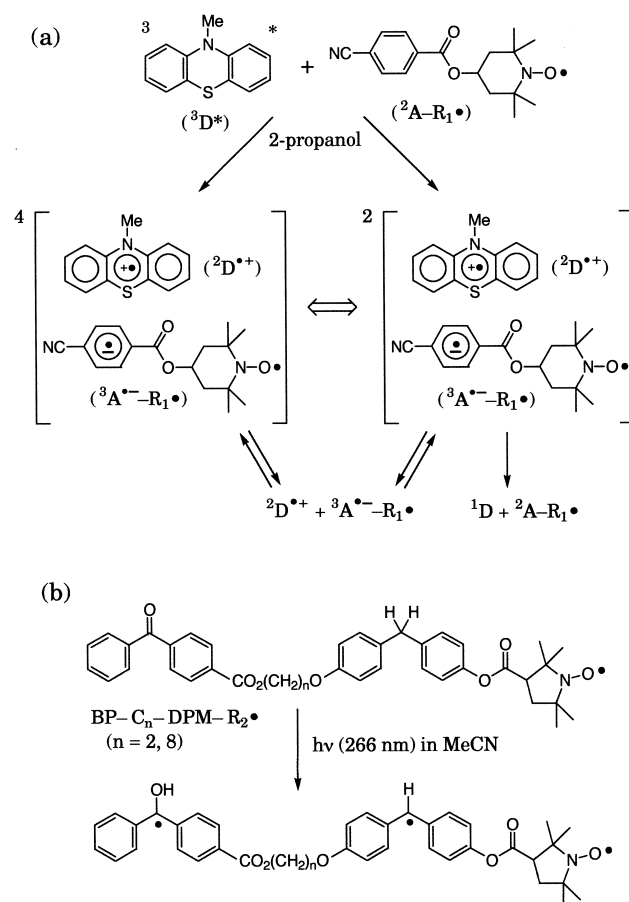


Fig. 7. Reaction schemes of three-spin systems observed for the electron transfer reaction of (a) triplet 10-methylphenothiazine ( $^3D^*$ ) with 4-(4-cyanobenzoyloxy)-TEMPO ( $^2A-R_1\cdot$ ) in 2-propanol and (b) for the photolysis of benzophenone(BP)-diphenylmethane(DPM)-nitroxide( $R_2\cdot$ ) trifunctional compounds in acetonitrile.

$R_1\bullet$ ) in 2-propanol.<sup>23</sup> Here,  $R_1\bullet$  is the TEMPO (2,2,6,6-tetramethylpiperidin-1-oxyl) radical. The reaction scheme is shown in Fig. 7a. As shown in this figure, the quartet ( $S = 3/2$ ) and doublet ( $S = 1/2$ ) states consisting of the cation radical ( ${}^2D^{\bullet+}$ ) and the anion biradical ( ${}^3A^{\bullet-}-R_1\bullet$ ) are generated after the electron transfer. From both of the quartet and doublet states, the radical and the biradical escape from solvent cages, forming the escape radical and biradical. On the other hand, the cage recombination only occurs from the doublet state, forming D and  ${}^2A-R_1\bullet$ .

We measured the  $A(t)$  profiles of the cation radical under magnetic fields of up to 10 T. From the profiles, we obtained the MFEs on the  $Y_E$  values. In Fig. 8a, we plot the  $R(B)(=Y_E(B)/Y_E(0\text{ T}))$  values observed with and without  $R_1\bullet$ . In the reaction without  $R_1\bullet$ , we can see from Fig. 8a that the  $R(B)$  value increases with increasing  $B$  for 0 T to 0.2 T and that the value decreases with increasing  $B$  from 0.2 T to 10 T. The maximum  $R(B)$  value is  $1.09 \pm 0.02$  at  $B = 0.2$  T. The magnetically induced increase and decrease in  $R(B)$  can be explained by the HFCM and the  $\Delta gM$ , respectively. In the reaction with  $R_2\bullet$ , we can see from Fig. 8a that the  $R(B)$  value increases with increasing  $B$  for 0 T to 2 T and that the value decreases with increasing  $B$  from 2 T to 10 T. The maximum  $R(B)$  value is as large as  $1.90 \pm 0.08$  at  $B = 2$  T. These MFEs can be explained by the RM, where the spin relaxation between the quartet-doublet states plays an important role during

the lifetime of the pair states.

We also studied the MFEs on reactions of triradicals generated by photolysis of benzophenone (BP)-diphenylmethane (DPM)-nitroxide( $R_2\bullet$ ) trifunctional compounds.<sup>24</sup> Here,  $R_2\bullet$  is the PROXYL (2,2,5,5-tetramethylpyrrolidin-1-oxyl) radical. The scheme of the reactions for BP- $C_n$ -DPM- $R_2\bullet$  ( $n = 2$  and 8) is shown in Fig. 7b. In this figure, we can see that a triradical is generated for each reaction. From the  $A(t)$  profiles at 345 nm, we obtained the MFEs on the decay rate of each triradical ( $k_{TR}$ ). Figure 8b shows the observed MFEs on the  $k_{TR}$  values for the triradicals generated from BP- $C_8$ -DPM- $R_2\bullet$ . We can see from this figure that the  $k_{TR}$  value observed in this reaction decreases with increasing  $B$  from 0 T to 2 T and that the value slightly increases with increasing  $B$  from 2 T to 10 T. We also found that the  $k_{TR}$  value observed in the reaction of BP- $C_2$ -DPM- $R_2\bullet$  decreased with increasing  $B$  from 0 T to 2 T and that the value increased with increasing  $B$  from 2 T to 10 T. These MFEs on  $k_{TR}$  can also be explained by the RM, where the spin relaxation between the quartet-doublet states plays an important role during the lifetime of the triradicals. The decay rate of the triradicals at  $B = 2$  T is about  $6 \times 10^6\text{ s}^{-1}$ , which is much larger than the decay rate of the corresponding biradicals at  $B = 2$  T (about  $1 \times 10^5\text{ s}^{-1}$ ). This increase is due to the enhancement of spin relaxation by  $R_2\bullet$ .

### 5. Spin Dynamics of Radical Pairs Studied with an Optically Detected ESR Apparatus

In the preceding sections, the studies of MFEs on radical reactions with the transient optical absorption ( $A(t)$  profiles) due to intermediate radicals were reviewed. Direct measurements of intermediate radicals with various ESR methods are also possible. For example, we first studied the radical pairs in micelles with a continuous wave (cw) ESR method without field modulation and found CIDEP signals due to spin-correlated radical pairs.<sup>25</sup> The cw-ESR method without field modulation is informative, but its time resolution is not always high enough to clarify the details of spin dynamics. Although pulsed-ESR methods such as the Fourier transfer (FT) ESR can improve the time resolution, they have many limitations in measuring spin dynamics. For example, such ESR methods can provide us only the combined information of concentration and polarization. Thus, an optical detected (OD) ESR method which is realized by the coupling of the pulsed-ESR and transient absorption methods seems to be advantageous to the study of dynamic behavior of intermediate radicals.

Recently, we constructed such an ODESR apparatus, combining a JEOL RSV 2000 X-band pulsed-ESR one with our ns-transient optical absorption one.<sup>26</sup> Because we could realize the world best sensitivity in our ODESR apparatus, we have been able to obtain novel fruits on spin dynamics of radical pairs with a short microwave pulse. In this section, several typical results obtained with our ODESR for the photoreduction of carbonyl and quinone molecules in micelles will be introduced. The scheme of these reactions is also represented by reactions 16–21 and the decay of radical pairs in the presence of a magnetic field ( $\sim 0.3$  T) can be represented by Eq. 10. In this equation, the fast decay component corresponds to the population ( $[M]$ ) of the mixed state (M) of  $S$  and  $T_0$  and the slow one to the population ( $[T_{\pm}]$ ) of the combined state ( $T_{\pm}$ ) of

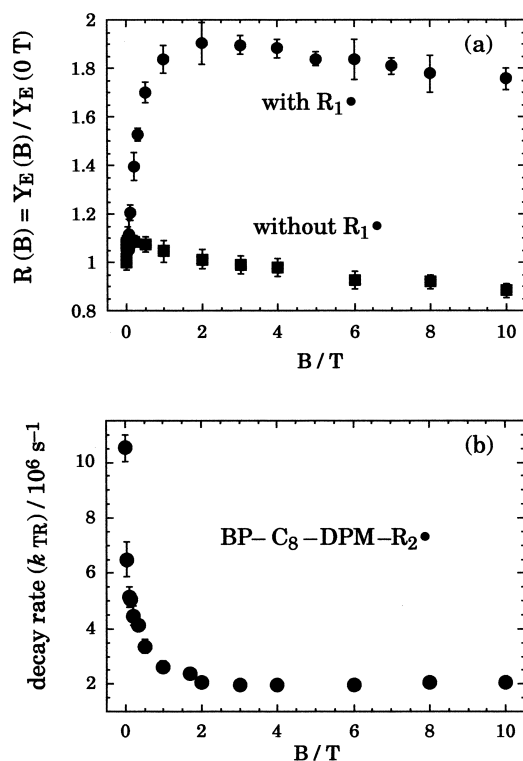


Fig. 8. (a) The  $R(B)(=Y_E(B)/Y_E(0\text{ T}))$  values observed for the electron transfer reaction of triplet 10-methylphenothiazine ( ${}^3D^*$ ) with 4-(4-cyanobenzoyloxy)-TEMPO ( ${}^2A-R_1\bullet$ ) in 2-propanol: (●) for the reaction system with  $R_1\bullet$  and (■) for the reaction system without  $R_1\bullet$ . (b) The MFEs on the decay rate ( $k_{TR}$ ) observed for the triradicals generated from BP- $C_8$ -DPM- $R_2\bullet$ .

$T_{+1}$  and  $T_{-1}$ .

Figure 9 shows typical  $A(t)$  profiles observed for a component radical without (curve a) and with (curve b) a microwave pulse whose width is 15 ns. In this figure, the origin of time ( $t = 0$  ns) corresponds to the laser-excitation and the time difference between the microwave pulse and laser one is represented by  $t_D$ . Upon laser-excitation of a carbonyl or quinone molecule (reaction 16), its triplet state is formed (reaction 17) in the ps-region. Thus, the initial stage of the  $A(t)$  profile corresponds to the generation of a radical pair (reaction 18) and its decay (reactions 19–21). When the microwave pulse is applied at  $t = t_D$ , a part of the population at the  $T_{\pm}$  state ( $C([T_{\pm}](t_D) - [M](t_D))$ ) is transferred to the M state.

$$[T_{\pm}](t_D + \varepsilon) = [T_{\pm}](t_D) - C([T_{\pm}](t_D) - [M](t_D)) \quad (29)$$

$$[M](t_D + \varepsilon) = [M](t_D) + C([T_{\pm}](t_D) - [M](t_D)) \quad (30)$$

After the application of the microwave pulse at  $t = t_D$ , the a–b curve shows a gradual rise and a slow decay after attaining its maximum at  $t = t_{M1}$ , as shown in Fig. 9. The initial rise corresponds to the disappearance of  $[M]$  with its rate constant ( $k_F$ ), as given by Eq. 12. In principle, this rate constant for radical pairs generated by the photoreduction of carbonyl and

quinone molecules in micelles can be obtained from their  $A(t)$  profiles with ns-laser photolysis measurements. In the actual measurements, however, this rate constant has never been obtained from their  $A(t)$  profiles because there are many components due to other species such as triplet precursors and reaction products in the profiles. From the present ODESER measurement, we could purely generate the mixed M state with the microwave pulse and succeeded in measuring the  $k_F$  value for the first time. Thus, this method can be called “Spin Manipulation.” From the decay of the a–b curve, the  $k_S$  value (see Eq. 13) can be obtained. We, therefore, could determine the  $k_P$  value for the first time from our ODESER method.<sup>26</sup>

$$k_P = 2(k_F - k_S) \quad (31)$$

After the decay of the a–b curve, this curve attains a constant value at  $t = t_E$  as shown in Fig. 9. This value corresponds to the yield of the escape radical. Thus, the rate constant of the spin-relaxation and that of the escape of radicals from a radical pair ( $k_R + k_R'$  and  $k_E$ ) can also be obtained with the following relations:

$$k_S = (k_R + k_R') + k_E \quad (13)$$

$$[a - b](t_E)/[a - b](t_{M1}) = k_E/k_S \quad (32)$$

The  $k_G$  and  $k_S$  values can also be obtained from the following method. When we measure the  $[a - b](t = t_E)$  value by changing the  $t_D$  value, we can obtain the bottom curve shown in Fig. 9. If  $t_D$  is negative, the  $[a - b](t = t_E)$  value becomes zero, because there is no radical pair at  $t = t_D$ . When  $t_D$  is increased from 0 ns, the  $[a - b](t = t_E)$  curve shows a fast rise and a slow decay after its maximum at  $t = t_{M2}$  as shown in Fig. 9. If the generation of the radical pairs is much faster than the disappearance from its mixed M state ( $k_G \gg k_F$ ), the initial part of the rise corresponds to the generation process with the rate constant of  $k_G$ . During this stage, the  $[M]/[T_{\pm}]$  ratio is kept approximately constant. When the generation of the radical pairs is slowed down due to the consumption of the triplet state, the  $[M]/[T_{\pm}]$  ratio is decreased by the cage recombination from the M state. On the other hand, the decay from the  $T_{\pm}$  state is much slower than that of the M one. Because the  $[M]/[T_{\pm}]$  ratio becomes zero at the maximum point ( $t = t_{M2}$ ), the decay part of the  $[a - b](t = t_E)$  curve corresponds to the decay of  $[T_{\pm}]$ . From its decay, therefore, the  $k_S$  value can also be obtained. This method for the determination of the  $k_S$  value is much better than that from the a–b curve mentioned before if the  $k_E$  value is much larger than the  $k_R + k_R'$  one.

It is noteworthy that all of the rate constants for the photoreduction of carbonyl and quinone molecules in micelles can accurately be determined from this ODESER method. From the usual laser photolysis method where only the  $A(t)$  profiles are used, the  $k_F$  value has not yet been measured and its accuracy in the determination of the other rate constants is much worse than that with this ODESER method. We have been carrying out such measurements for many reactions with this ODESER method and have determined all of their rate constants very precisely. The details of such studies will be published in the near future,<sup>27</sup> but typical results are shown in Table 1. Here, the rate constants determined at room temperature with our

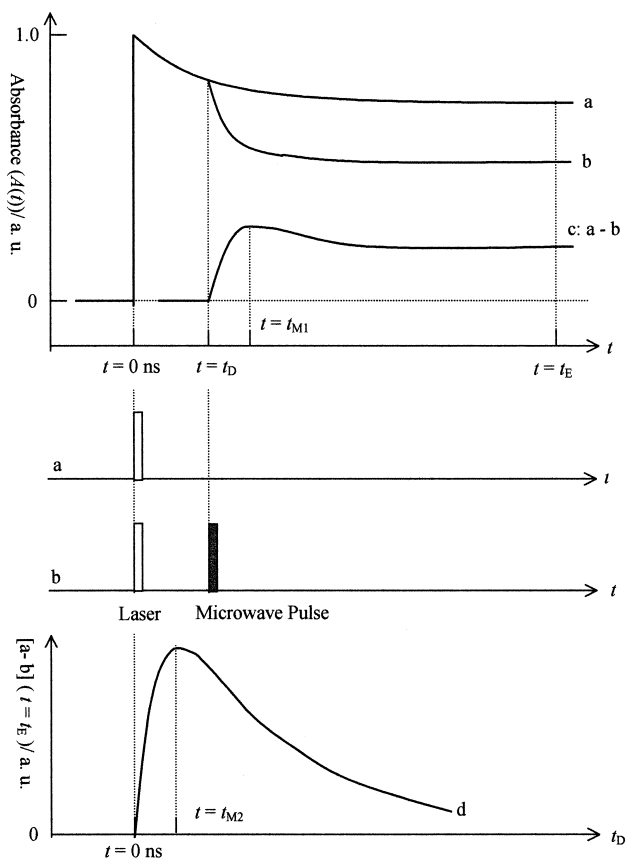


Fig. 9. (a)  $A(t)$  curve obtained at  $B = 331$  mT without microwave irradiation; (b)  $A(t)$  curve obtained at  $B = 331$  mT with short microwave pulse irradiation at  $t = t_D$ ; (c) Difference of the  $A(t)$  curves (trace a–trace b); (d)  $[a - b]$  value observed at  $t = t_E$  as a function of  $t_D$ .



Table 1. Rate Constants Determined with an ODESr Method at  $B = 331$  mT for Photoreduction of Several Carbonyl and Quinone Molecules (XCO) in Micelles (RH) at Room Temperature<sup>26,27</sup>

| XCO                | RH                    | $k_G$ <sup>a)</sup><br>$10^7 \times s^{-1}$ | $k_P$ <sup>b)</sup><br>$10^7 \times s^{-1}$ | $k_R + k_R'$ <sup>c)</sup><br>$10^5 \times s^{-1}$ | $k_E$ <sup>d)</sup><br>$10^5 \times s^{-1}$ |
|--------------------|-----------------------|---|---|--|---|
| MNQ <sup>e)</sup>  | SDS <sup>f)</sup>     | 3.3   | 1.5   | 3.3  | 5.8   |
| BP <sup>g)</sup>   | SDS <sup>f)</sup>     | 0.4   | 1.9   | 3.3  | 2.1   |
| BP <sup>g)</sup>   | Brij 35 <sup>h)</sup> | 0.8   | 0.6   | 2.2  | 1.1   |
| DFBP <sup>i)</sup> | SDS <sup>f)</sup>     | 4.3   | 1.8   | 8.0  | 0.5   |
| DFBP <sup>i)</sup> | Brij 35 <sup>h)</sup> | 5.2   | 0.6   | 3.8  | 0.5   |

a) See reaction 18. b) See Eq. 12 and reaction 21. c) See Eqs. 13–15. d) See Eq. 13 and reaction 20. e) 2-Methyl-1,4-naphthoquinone. f) Sodium dodecyl sulfate. g) Benzophenone. h)  $\alpha$ -Dodecyl- $\omega$ -hydroxypolypoly(oxyethylene). i) Decafluorobenzophenone.

ODESR method at  $B = 331$  mT for the photoreduction of 2-methyl-1,4-naphthoquinone (MNQ), BP, and DFBP in micellar SDS and Brij 35 solutions are listed.<sup>26,27</sup> From this table, we can see the following features in the spin dynamics of these reactions: 1) The rates of hydrogen abstraction ( $k_G$ ) of MNQ and DFBP are about ten times larger than those of BP. This is due to the fact that the  $n, \pi^*$  characters of  $^3\text{MNQ}^*$  and  $^3\text{DFBP}^*$  are larger than that of  $^3\text{BP}^*$ . 2) The rates of cage recombination ( $k_P$ ) in the SDS micellar solution are about three times larger than those in the Brij 35 solution. This is due to the fact that the SDS micelles are smaller than the Brij 35 ones. 3) The rates of triplet spin relaxation ( $k_R + k_R'$ ) of DFBP are slightly larger than those of MNQ and BP. This is due to the fact that the anisotropic Zeeman and HFC terms of the three kinds of radical pairs are similar to one another. The fact that the  $k_R + k_R'$  values of DFBP are slightly larger than those of MNQ and BP may be due to the effect of ten F-atoms. 4) The rates of radical escape ( $k_E$ ) have the increasing order of  $k_E(\text{MNQ}) > k_E(\text{BP}) > k_E(\text{DFBP})$ . This can be explained by the increasing order of the hydrophilicity of the MNQ semiquinone, BP ketyl, and DFBP ketyl radicals. The MFEs on the  $\tau_{RP}$  and  $Y_E$  values under ultrahigh fields described in Section 3 correspond well to features 3 and 4 obtained in this section.

The above-mentioned results clearly show that the ODESr method gives unique and accurate knowledge on spin dynamic of radical pairs. It is noteworthy that this method is also used for the studies of novel phenomena of radical pairs such as quantum beat<sup>28</sup> and level-crossing.<sup>29</sup> A weak point of ODESr is the fact that its measurements have been limited to the X-band microwave ( $\nu \sim 9$  GHz,  $B \sim 0.31$  T). This means that the spin dynamics can only be measured at  $B \sim 0.3$  T. At present, it is very difficult for us to construct ODESr apparatus at various microwave frequencies because the microwave amplifier is only available at X and K band regions. We are now developing a K-band ODESr apparatus (at  $B \sim 0.62$  T) for the first time in the world.<sup>30</sup>

## 6. Concluding Remarks

Using superconducting ( $B \leq 10$  T) and pulsed ( $B \leq 30$  T) magnets, we found several new MFEs not only in micellar solutions but also in nonviscous ones. We studied MFEs on the escape radical yield ( $Y_E$ ) for the photoreduction of 4-methoxybenzophenone with thiophenol in various nonviscous solu-

tions. We found that the  $R(B) = Y_E(B)/Y_E(0 \text{ T})$  value was decreased with increasing  $B$  from 0 T to 30 T. The  $1 - R(B)$  value was proportional to  $B^{1/2}$  in a low field region ( $B < 4$  T), but was almost saturated above 20 T. To the best of our knowledge, this is the first observation of the saturation of MFEs due to the isotropic  $\Delta g$  mechanism. We have successfully interpreted these saturated MFEs in terms of the modified diffusion model.

We also studied MFEs on the radical pair lifetime ( $\tau_{RP}$ ) and the escape radical yield ( $Y_E$ ) for the photoreduction of carbonyl and quinone compounds in the micellar solutions of SDS and Brij 35. The  $\tau_{RP}$  and  $Y_E$  values were found to increase with increasing  $B$  from 0 T to 2–3 T and to show saturation or reversion at  $B = 2$  T, but the reversion was found to be saturated at  $B \sim 30$  T. These MFEs were explained in terms of the relaxation mechanism due to the anisotropic dipole–dipole, Zeeman, and HFC interactions. Using our ODESr apparatus, we studied the spin dynamics for the radical pairs generated from the photoreduction of carbonyl and quinone compounds in the micellar solutions of SDS and Brij 35 and obtained all necessary rate constants of these reactions at  $B \sim 0.3$  T very precisely. These rate constants obtained with this ODESr method are very useful in the analysis of the MFEs on the  $\tau_{RP}$  and  $Y_E$  values under ultrahigh fields of up to 30 T.

Ordinary MFEs on chemical reactions through radical pairs and biradicals are due to the spin conversion between their singlet-triplet states. Recently, we have first found large MFEs in several reaction systems where three odd electrons appear in radical-biradical pairs and chain-linked triradicals. Such large MFEs observed in nonviscous solutions can be explained by the relaxation mechanism where their doublet-quartet conversion plays an important role.

## Abbreviations

|                     |  |
|---------------------|--|
| A                   | electron acceptor                                |
| $A(t)$ profile      | time profile of transient absorption             |
| BP                  | benzophenone                                     |
| BP- <sup>13</sup> C | [carbonyl- <sup>13</sup> C]benzophenone          |
| BP- $d_{10}$        | benzophenone- $d_{10}$                           |
| CIDEP               | chemically induced dynamic electron polarization |
| CIDNP               | chemically induced dynamic nuclear polarization  |
| D                   | electron donor                                   |

|                  |   |
|------------------|---|
| AgM              | Ag mechanism  |
| DFBP             | decafluorobenzophenone                                |
| DPM              | diphenylmethane                                       |
| HFC              | hyperfine coupling                                    |
| HFCM             | hyperfine coupling mechanism                          |
| LCM              | level-crossing mechanism                              |
| MFE              | magnetic field effect                                 |
| MIE              | magnetic isotope effect                               |
| MNQ              | 2-methyl-1,4-naphthoquinone                           |
| NQ               | 1,4-naphthoquinone                                    |
| ODESR            | optical detected ESR                                  |
| R•               | radical generated from RH                             |
| R <sub>1</sub> • | TEMPO (2,2,6,6-tetramethylpiperidin-1-oxyl) radical   |
| R <sub>2</sub> • | PROXYL (2,2,5,5-tetramethylpyrrolidin-1-oxyl) radical |
| RH               | hydrogen donor  |
| RM               | relaxation mechanism                                  |
| S–T conversion   | singlet-triplet conversion                            |
| $\tau_{RP}$      | radical pair lifetime                                 |
| $Y_E$            | escape radical yield                                  |
| XCO              | carbonyl or quinone molecule                          |
| XCOH•            | ketyl or semiquinone radical                          |

The authors thank the other members of Molecular Photochemistry Laboratory of RIKEN, Dr. S. Ikeda, Dr. K. Nishizawa, Dr. Y. Mori, Dr. M. Igarashi, Dr. A. D. Astashkin, B. M. Tadjikov, and J. R. Woodward for their collaboration in measuring MFEs and spin dynamics. They also thank Dr. H. Abe and Dr. G. Kido of NRIM (National Research Institute for Metals) for their collaboration in making a pulsed magnet which is suitable for the studies of chemical reactions in solutions. They express their sincere gratitude to Prof. K. Salikhov of Zavoisky Physical-Technical Institute, Russia, and Prof. J. B. Pedersen of Odense University, Denmark, for their helpful discussions on theoretical interpretations of their MFEs and spin dynamics. This work was supported by the MR (magnetic resonance) Science Project of RIKEN together with many other funds supplied to the authors by RIKEN and the Ministry of Education, Science, Sports and Culture.

## References

- 1 H. Hayashi, in "Dynamic Spin Chemistry," ed by S. Nagakura, H. Hayashi, and T. Azumi, Kodansha/Wiley, Tokyo/New York, (1998), Chap. 2, p. 7, and references cited therein.
- 2 S. Nagakura, in "Dynamic Spin Chemistry," ed by S. Nagakura, H. Hayashi, and T. Azumi, Kodansha/Wiley, Tokyo/New York (1998), Chap. 1, p. 1.
- 3 H. Hayashi, K. Itoh, and S. Nagakura, *Bull. Chem. Soc. Jpn.*, **39**, 199 (1966); K. Itoh, H. Hayashi, and S. Nagakura, *Mol. Phys.*, **17**, 561 (1969).
- 4 H. Hayashi and S. Nagakura, *Bull. Chem. Soc. Jpn.*, **57**, 322 (1984).
- 5 Y. Tanimoto, H. Hayashi, S. Nagakura, H. Sakuragi, and K. Tokumaru, *Chem. Phys. Lett.*, **41**, 267 (1976); H. Hayashi and S. Nagakura, *Bull. Chem. Soc. Jpn.*, **51**, 2862 (1978).
- 6 Y. Sakaguchi and H. Hayashi, *Chem. Lett.*, **1993**, 1183.
- 7 K. Nishizawa, Y. Sakaguchi, H. Hayashi, H. Abe, and G. Kido, *Chem. Phys. Lett.*, **267**, 501 (1997).
- 8 D. Bürstner, H.-J. Wolff, and U. E. Steiner, *Angew. Chem., Int. Ed. Engl.*, **17**, 33 (1994).
- 9 M. Wakasa, K. Nishizawa, H. Abe, G. Kido, and H. Hayashi, *J. Am. Chem. Soc.*, **121**, 9191 (1999), and references cited therein.
- 10 S. G. Boxcer, C. E. D. Chidsey, and M. G. Roelofs, *J. Am. Chem. Soc.*, **104**, 1452 (1982).
- 11 K. Schulten and I. R. Epstein, *J. Chem. Phys.*, **71**, 309 (1979).
- 12 J. H. Freed, in "Chemically Induced Magnetic Polarization," ed by L. T. Muus, P. W. Atkins, K. A. McLauchlan, and J. B. Pedersen, D. Reidel, Dordrech (1977), Chap. 19, 309.
- 13 P. W. Atkins, in "Chemically Induced Magnetic Polarization," ed by L. T. Muus, P. W. Atkins, K. A. McLauchlan, and J. B. Pedersen, D. Reidel, Dordrech (1977), Chap. 11, 191.
- 14 Terazima, K. Okamoto, and N. Hirota, *J. Phys. Chem.*, **97**, 13387 (1993).
- 15 M. Wakasa and H. Hayashi, *Chem. Phys. Lett.*, **327**, 343 (2000).
- 16 Y. Sakaguchi, S. Nagakura, A. Minoh, and H. Hayashi, *Chem. Phys. Lett.*, **82**, 213 (1981); Y. Sakaguchi, H. Hayashi, and S. Nagakura, *J. Phys. Chem.*, **86**, 3177 (1982).
- 17 Sakaguchi and H. Hayashi, *Chem. Phys. Lett.*, **87**, 539 (1982).
- 18 Y. Fujiwara, K. Yoda, T. Aoki, and Y. Tanimoto, *Chem. Lett.*, **1997**, 435.
- 19 Y. Fujiwara, Y. Taga, T. Tomonari, Y. Akimoto, T. Aoki, and Y. Tanimoto, *Bull. Chem. Soc. Jpn.*, **74**, 237 (2001).
- 20 H. Hayashi, Y. Sakaguchi, M. Wakasa, Y. Mori, and K. Nishizawa, *Appl. Magn. Reson.*, **18**, 307 (2000), and references cited therein.
- 21 K. Nishizawa, Y. Sakaguchi, H. Abe, G. Kido, and H. Hayashi, *Mol. Phys.* to be published.
- 22 Y. Fujiwara, R. Nakagaki, and Y. Tanimoto, in "Dynamic Spin Chemistry," ed by S. Nagakura, H. Hayashi, and T. Azumi, Kodansha/Wiley, Tokyo/New York (1998), Chap. 3, p. 49.
- 23 Y. Mori, Y. Sakaguchi, and H. Hayashi, *Chem. Phys. Lett.*, **286**, 446 (1998); Y. Mori, Y. Sakaguchi, and H. Hayashi, *J. Phys. Chem. A*, **104**, 4896 (2000).
- 24 Y. Mori, Y. Sakaguchi, and H. Hayashi, *Chem. Phys. Lett.*, **301**, 365 (1999).
- 25 Y. Sakaguchi, H. Hayashi, H. Murai, and Y. J. I'Haya, *Chem. Phys. Lett.*, **110**, 275 (1984).
- 26 Y. Sakaguchi, A. V. Astashkin, and B. M. Tadjikov, *Chem. Phys. Lett.*, **280**, 481 (1997).
- 27 J. R. Woodward and Y. Sakaguchi, *J. Phys. Chem. A*, in press.
- 28 B. M. Tadjikov, A. V. Astashkin, and Y. Sakaguchi, *Chem. Phys. Lett.*, **283**, 179 (1998).
- 29 B. M. Tadjikov, A. V. Astashkin, and Y. Sakaguchi, *Chem. Phys. Lett.*, **284**, 214 (1998).
- 30 Y. Sakaguchi, to be published.



Hisaharu Hayashi was born in Tokushima in 1942. He has been the Director of Molecular Photochemistry Laboratory at RIKEN (The Institute of Physical and Chemical Research) since 1983. He graduated from the University of Tokyo in 1964 and received his Dr. Sc. under the auspices of Prof. Saburo Nagakura at The Institute for Solid State Physics of the University of Tokyo in 1969. Since 1969, he has been working in RIKEN. He was appointed as a visiting professor at the Institute for Molecular Science for two years (1984/1986). He has been a visiting professor at Department of Electronic Chemistry of Interdisciplinary Graduate School of Science and Engineering of Tokyo Institute of Technology since 1997. His research interests are in Spin Chemistry, including magnetic field effects on chemical reactions. In 1998, he edited a book entitled "Dynamic Spin Chemistry" with Prof. Saburo Nagakura and Prof. Tohru Azumi. He received the Award of Chemical Society of Japan for Young Scientists in 1976 and the Award of Japanese Photochemistry Association in 1992.



Yoshio Sakaguchi was born in Tokyo in 1954. He has been a member of Molecular Photochemistry Laboratory at RIKEN (The Institute of Physical and Chemical Research) since 1983 and has been promoted to its Senior Scientist in 1991. He was graduated from the University of Tokyo in 1976 and received his Dr. Sc. under the auspices of Prof. Saburo Nagakura at the Institute for Solid State Physics of the University of Tokyo in 1981. He had been a visiting associate professor at the Department of Material Science of Graduate School of Science and Engineering of Saitama University since 1993 and has been promoted to a visiting professor since 1999. His research interests are in Spin Chemistry, including magnetic field and microwave field effects on chemical reactions.



Masanobu Wakasa was born in Tokyo in 1961. He graduated from Gakushuin University in 1985 and received his Dr. Sc. from Gakushuin University (Prof. K. Mochida) in 1989. He was given the Research Fellowship for Young Scientists from Japan Society for the Promotion of Science (1988/1989). He has been a member of Molecular Photochemistry Laboratory at RIKEN (The Institute of Physical and Chemical Research) since 1989 and has been promoted to its Senior Research Scientist since 1999. His research interests are in photochemistry and organometallic chemistry. In 1991, he received the Award for Young Chemists from the Silicon Photochemistry Society of Japan.